



Sorption of methylene blue on iodate-chitosan assembled composite from aqueous solution

Aloysius Akaangee Pam^{a,*}, Sesugh Ande^b, Ishaq S. Eneji^b, Rufus Sha'Ato^b

^aDepartment of Chemistry, Faculty of Science, Federal University Lokoja, Lokoja, Nigeria,
email: aloysius.pam@fulokoja.edu.ng (A.A. Pam)

^bDepartment of Chemistry and Center for Agrochemical Technology, University of Agriculture, Makurdi, Nigeria,
email: sesughande@gmail.com (S. Ande) eneji3@yahoo.com (I.S. Eneji), rshaato@gmail.com (R. Sha'Ato)

Received 7 July 2018; Accepted 23 May 2019

ABSTRACT

This study focused on the synthesis of chitosan composite using potassium iodate, KIO_3 for the adsorption of methylene blue (MB) in water. The physicochemical properties of the obtained adsorbent were characterized by Brunauer-Emmett-Teller (BET) surface area technique, Fourier transform infrared (FTIR) spectroscopy, scanning electron microscope (SEM) and X-ray diffraction (XRD). The effect of adsorption parameters such as adsorbent dosage, initial concentration, pH and temperature are systematically explored *via* adsorption batch method. The experimental results showed that the adsorption process was spontaneous and exothermic in nature and kinetically and isothermally fitted pseudo-second order kinetic and Langmuir models, respectively. In addition, the estimated maximum monolayer adsorption capacity of I-IC was 109 mg/g. The reuse ability of the I-IC was established with 3 successive cycles of adsorption-desorption. This indicates that the I-IC can be used as a low-cost and effective adsorbent for dye treatment in water.

Keywords: Chitosan; Iodate incorporated chitosan; Adsorption; Regeneration; Methylene blue

1. Introduction

Synthetic dyes are among the common pollutants frequently discharged from many industries into the environment. Most of these dyes are toxic, carcinogenic, in addition, recalcitrant and thus stable in the receiving environment thereby posing serious threat to human health and aquatic animals [1]. Methylene blue is a typical cationic dye that is widely applied in dyeing silk, leather, paper, wool, and cotton in industry [2]. Discharging of this dye into water bodies is harmful to humans as it can cause nausea, vomiting, profuse sweating, diarrhoea, gastritis, mental confusion, eye/skin irritation and systemic effect including cyanosis and blood changes [3]. Chitosan is widely used for the removal of different kinds of dyes, particularly the cationic ones because of the amino and hydroxyl groups of chitosan [4]. However, the powdery chitosan has some disadvantages

that hampers its practical application; it is easily dissolves under acidic conditions and has poor mechanical strength [5]. Interestingly, the amino groups in chitosan can easily be chemically modified [6] to improve its binding and selectivity toward dyes. In addition, the blending of chitosan with other materials, especially those with fast treatment prospects can be applied in environmental removal of dyes. Many studies have evaluated dye removal using different materials incorporated with chitosan. For example, Li et al. [7] removed methylene blue from aqueous systems by chitosan coated magnetic mesoporous silica nanoparticles, equally, cross-linked chitosan/sepiolite composite was applied for the adsorption of methylene blue and reactive orange 16F by Marrakchi et al. [8]. Also, Wang et al. [9] used chitosan-g-poly (acrylic acid)/attapulgitite composite for fast removal of methylene blue from aqueous solution. Moreover, chemicals such as potassium iodate (KIO_3) and sodium iodate ($NaIO_3$) have been incorporated into sorbents for the removal of cationic metals in aqueous media.

*Corresponding author.

However, the number of studies investigating the adsorption of these pollutants on iodate-incorporated materials is extremely limited. Chubar et al. [10] treated cork powder with sodium iodate for removal of Cu(II), Zn(II) and Pb(II) in aqueous solution, while Gedam and Dongre [6] tested the potential of KIO₃-chitosan composite for Pb(II) removal in aqueous solution as well as its regeneration. To our knowledge, there have been no studies on the adsorption capacity of MB using a KIO₃-chitosan assembled composite. Hence, KIO₃-chitosan composite was synthesized in this work to determine whether there is any significant influence of the iodate on the cationic dye (methylene blue) removal. In the present study, we have investigated the adsorption capability of iodate-chitosan assembled composite towards the removal of methylene blue (MB) in aqueous solution. Adsorption isotherm and kinetic models were also investigated under different conditions (solution pH, adsorbent dose, initial dye concentration, and solution temperature) in order to enhance the removal of the dye.

2. Materials and methods

2.1. Synthesis of iodate-incorporated chitosan (I-IC) composite

The chitosan composite was prepared using similar approach reported in [6]. Briefly, 1.0 g of chitosan (medium molecular weight with degree of deacetylation, 75–80%, Sigma Aldrich) was dissolved in 100 mL acetic acid (2%) followed by stirring at 50°C for 30 min to obtain homogeneous gel. Parallely, a previous prepared solution of Potassium iodate (KIO₃) dissolved in anhydrous ethanol (2:1 w/w) was mixed with chitosan gel in (1:1 w/w) and the mixture was homogenized for 5 h at 500 rpm. This mixture was added drop-by-drop into a solution of 50% aqueous ammonia and allowed to stand for 30 min. The composite was filtered and subsequently washed with water, and oven-dried at 60°C for 24 h. Finally, it was ground, sieved to 200 mesh sizes, stored in sample bottle for further sorption experiment.

2.2. Characterization of the adsorbent

The specific surface area (m²/g) (BET method) and porosity (Barrett–Joyner–Halenda (BJH) method) was by N₂ adsorption (Micromeritics 3 Flex, USA). The micromorphology of the adsorbent was examined using FESEM (FEI Nova 230) operating at an accelerating voltage of 80 kV. The elemental composition was achieved by Energy dispersive X-ray (EDX) coupled with high-resolution FEI Nova 230 FESEM. To investigate the crystallinity of the I-IC, XRD analysis was conducted on an X-ray diffractometer (Bruker/ D5000, Germany). Diffraction patterns were recorded over the angular range of 10–80° 2θ using Cu-Kα radiation (k = 1.5406 Å) operated at 15 kV and 30 mA, using a slit width of 0.2 and scan speed of 1°/min for all scans. Thermogravimetric analyzer (STA 600 Perkin Elmer) investigated the pyrolysis behaviour of the PC and I-IC over the temperature range of (0–900°C) at a heating rate of 10°C/min under N₂ flow. The samples were dried to a constant weight, the ground samples (approximately 18 mg) were placed on top of the attenuated total reflection (ATR) crys-

tal using a mechanical anvil, and spectra were collected between 4000 cm⁻¹ and 400 cm⁻¹ at a resolution of 4 cm⁻¹ averaging 32 scans per sample. The spectra were collected in transmittance mode in triplicate, and the average value was used.

The pH of zero point charge (pH_{ZPC}) was determined based on the method described in [11]. The pH at the pH_{ZPC} of I-IC was measured by using the pH drift method. The pH of 0.1 mol/dm³ NaCl solution was adjusted between 2–12 by adding either HCl or NaOH. Then, 0.1 g of the I-IC was added to 40 mL of respective pH solution, the mixture was agitated on an orbital shaker for 24 h at room temperature to attain equilibrium. The final suspension pH was again measured using pH meter, and the initial and final pH values were plotted to determine the pH_{ZPC}.

2.3. Adsorption experiment

The stock solution for MB (1000 mg/L) was prepared by dissolving 1.00 g of methylene blue (Merck, Germany) in 1 L of ultra pure water. The stock solution was subsequently diluted to obtain the working concentrations.

The adsorption experiments were operated by batch mode considering parameters such as adsorbent dosage 0.08–0.3 g, initial dye concentration 20–80 mg/L, pH 2–8 and temperature 30–40°C. In order to ensure good contact between the dye and the I-IC, the dispersions in the flasks were shaken at 150 rpm for 70 min in a constant temperature water bath shaker (Mettler WNB 10, Germany). The final supernatants were determined by UV spectrometer (Perkin-Elmer lambda 25) at a maximum wavelength of 640 nm. The MB retained in the adsorbent phase (q_e , mg/g) and percentage of removal (%) were calculated by using Eqs. (1) and (2).

$$q_e = \frac{V(C_o - C_e)}{M} \quad (1)$$

$$\text{Percentage of removal (R)} = \frac{(C_o - C_e)}{C_o} \times 100 \quad (2)$$

where C_o and C_e represent the initial and equilibrium concentrations of MB (mg/L), V is the volume (L) of solution used, and M the weight of adsorbent (g). All adsorption experiments were carried out in duplicate.

3. Results and discussions

3.1. Adsorbent characterization

Elemental analysis and pore structural parameters of I-IC are as presented in Table 1. The elemental analysis confirmed the presence of C (21.25%), N (24.24%), O (38.24) and K (16.27%). The N₂ adsorption/desorption isotherm (Fig. 1b), revealed that the isotherm is of type IV (from IUPAC classification), with a hysteresis loop at higher relative pressure, signifying the presence of mesopore [12]. Besides, the specific surface area, pore volume, and average pore diameter were 1.4991 m²/g, 0.173 cm³/g and 21.71 nm. The small surface area of the I-IC adsorbent is related to the big sized mesopores and the small pore

Table 1
Elemental analysis and pore structural parameters of I-IC

Sample	SBET (m ² /g)	V _{total} (cm ³ /g)	Average pore diameter (nm)	Element (wt%)			
				C	N	O	K
I-IC	1.499	0.173	21.712	21.25	24.24	38.24	16.27

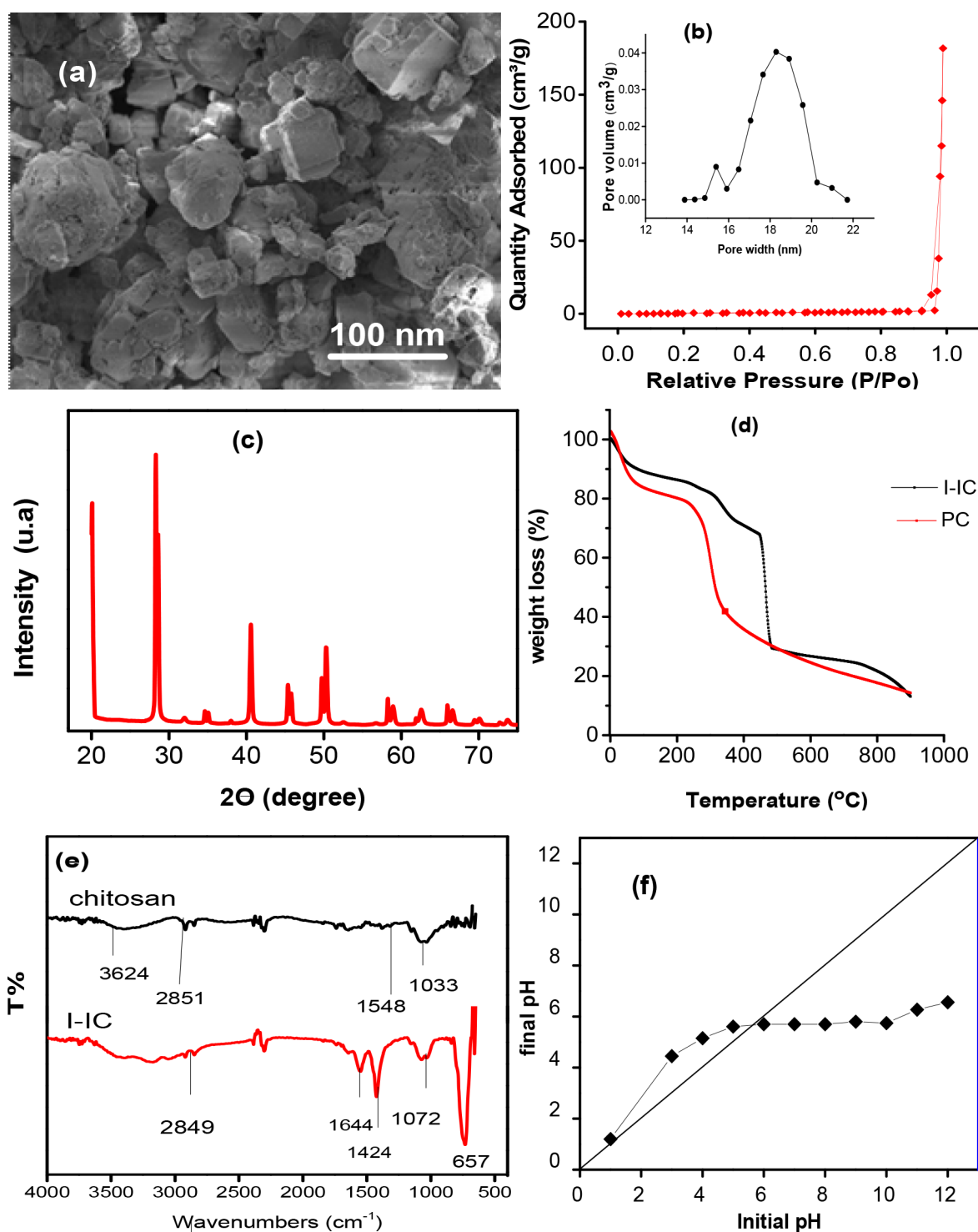


Fig. 1. (a) SEM images and (b) BJH pore size distribution (c) XRD pattern of synthesized.

volume. The chemical composition of the chitosan (PC) and I-IC were both investigated by FT-IR spectroscopy as presented in Fig. 1e. The major bands for the pure chitosan can be assigned as follows: 2851 cm^{-1} (CH- stretching vibration), 3624 cm^{-1} (NH, -OH stretch), 1033 cm^{-1} (C-O stretching vibration in -COH). Compared to the spectrum of the PC, that of the I-IC exhibits new adsorption bands and shift to lower or higher frequencies, along with new peaks at 657 cm^{-1} and 1652 cm^{-1} indicate the presence of iodate compound and NH bending vibration in NH_2 group, respectively. The above identified peaks in PC after treatment with iodate, were observed to shift to 2849 cm^{-1} , and 1072 cm^{-1} , correspondingly.

The powdered XRD pattern of the synthesized I-IC is shown in Fig. 1c. The XRD diffractogram of the material showed sharp narrow peaks, indicating that the samples was well crystallized. The peaks correspond to 2θ values of 20.1, 28.3°, 35.0°, 40.7°, 45.9° and 49.1° corresponding to miller indices of (111), (002), (220), (022), (121) and (220). All the peaks are indexed to potassium iodate and matched well with the standard card (JCPDS no. 01-072-1955) and in good agreement with that reported in [13]. In order to verify the I-IC crystallinity, the Debye-Scherrer equation [Eq. (3)] was used with respect to highly intensified peak [14].

$$\text{Mean crystallite size } (D) = \frac{0.89\lambda}{\beta \cos\theta} \quad (3)$$

where $\lambda = 1.540562 \text{ \AA}$, β = broadening of width at the half-peak height (WHPH) in radian, and θ = Bragg angle, respectively. An average particle diameter of 68.55 nm was reported indicating that KIO_3 in the chitosan composite was properly crystallized.

The thermal stability of the chitosan (PC) and I-IC is shown in Fig. 1d. The incorporated iodate shows considerable influence on the pyrolysis of the chitosan. For instance, the decomposition of the composite shifts to a relatively higher temperature above the temperature of 650°C, the release of volatile were strongly hindered, only 70.4% was lost against 96.8%. Furthermore, the maximum degradation state was accomplished by a weight loss of 75.4% (in absence of KIO_3) and 11.35% (in the presence of KIO_3) for the second stage of decomposition. This is because the iodate has been implanted onto the chitosan.

3.2. Effect of adsorbent dosage

To optimize the interaction between the dye molecules and adsorption sites of the I-IC in solution, the I-IC weight was varied from 0.08 to 0.3 g using initial dye concentration of 50 mg/L.

The result of the removal percentage of dye molecules at different doses of I-IC is presented in Fig. 2a. As the I-IC concentration was varied from 0.08 to 0.3 g, the removal efficiency of dye increased from 90.9 to 93.0%. This increase in adsorption was ascribed to the increase in the number of available sorption sites on the surface of the I-IC. Above 0.18 g of I-IC dose, there was no significant removal rate. Consequently, subsequent batch experiments were carried out using adsorbent dosage of 0.18 g. A similar result has been reported in literature [15].

3.3. Effect of time and initial MB concentration

Fig. 2b shows the adsorption equilibrium time for the removal of the cationic dye on I-IC.

Results show that the uptake of MB dye was rapid at the beginning (first 40 min) and then continued to increase as the adsorption proceeds until reaching equilibrium after 60 min. The behavior is due to the presence of numerous adsorption sites on the I-IC surface in the initial stage of the reaction, which gradually is saturated with the MB at increasing contact time. By increasing the dye initial concentration from 20 to 80 mg/L, the dye removal rate decreased from 97.6 to 93.4%. This is because at higher initial concentration of the dye, there are limited number of sorption centers on the sorbent, therefore, feasible adsorption becomes dependent on initial concentration, which was similarly reported by Zhang et al. [16]. The effect of time is an important parameter in adsorption studies especially for practical water treatment [17]. In this study, the time required to reach equilibrium was fast, indicating feasibility properties of the adsorbent and its excellent affinity towards the MB.

3.4. Effect of pH

It is recognized that the pH of the solution can affect the surface charge of the adsorbent, the extent of ionization of dyes, as well as the structure of dye molecules [18]. The effect of pH on adsorption of MB was investigated using 80 mg/L of dye. It can be seen from Fig. 2c that with an increase in alkalization of the solution there was a positive effect on MB removal. The percentage removal of the dye was significantly increased above pH 6 and attained maximum removal around pH 8 (94.4%); subsequently, no significant change was observed. This observation should be attributed to the I-IC pH_{ZPC} . By taking into consideration that the pH_{ZPC} of I-IC surface is 6.0, it is assumed that a negative charge developed on its surface at pH above pH_{ZPC} and a positive charge below that value. Therefore, it is expected that the adsorption of MB on the surface of I-IC will be favored for solution $\text{pH} > 6.0$ where increased electrostatic interactions may occur. The observation is similar to previous studies as MB is a cationic dye and its adsorption is favoured at basic pH [19].

3.5. Effect of temperature on the adsorption of MB

A study of the temperature dependence of the adsorption processes gives valuable information about the enthalpy and entropy changes accompanying adsorption [20]. Therefore, the effect of temperature on the removal of MB from aqueous solutions was further examined under optimized conditions, keeping I-IC dose, contact time, initial concentration, shaken speed and solution volume constant. Increasing the solution temperature decreased the percentage of MB removal from 96.1% to 92.0%. Besides, the solution temperature did not show significant dye removal when compared with interacting the dye and the I-IC dose (Fig. 2d) at room temperature, which means investigating the dye adsorption at room temperature was sufficient. Moreover, this parameter was not found to have such a substantial influence in MB adsorption as compared to pH or I-IC dose. Most of the adsorption process involving dyes

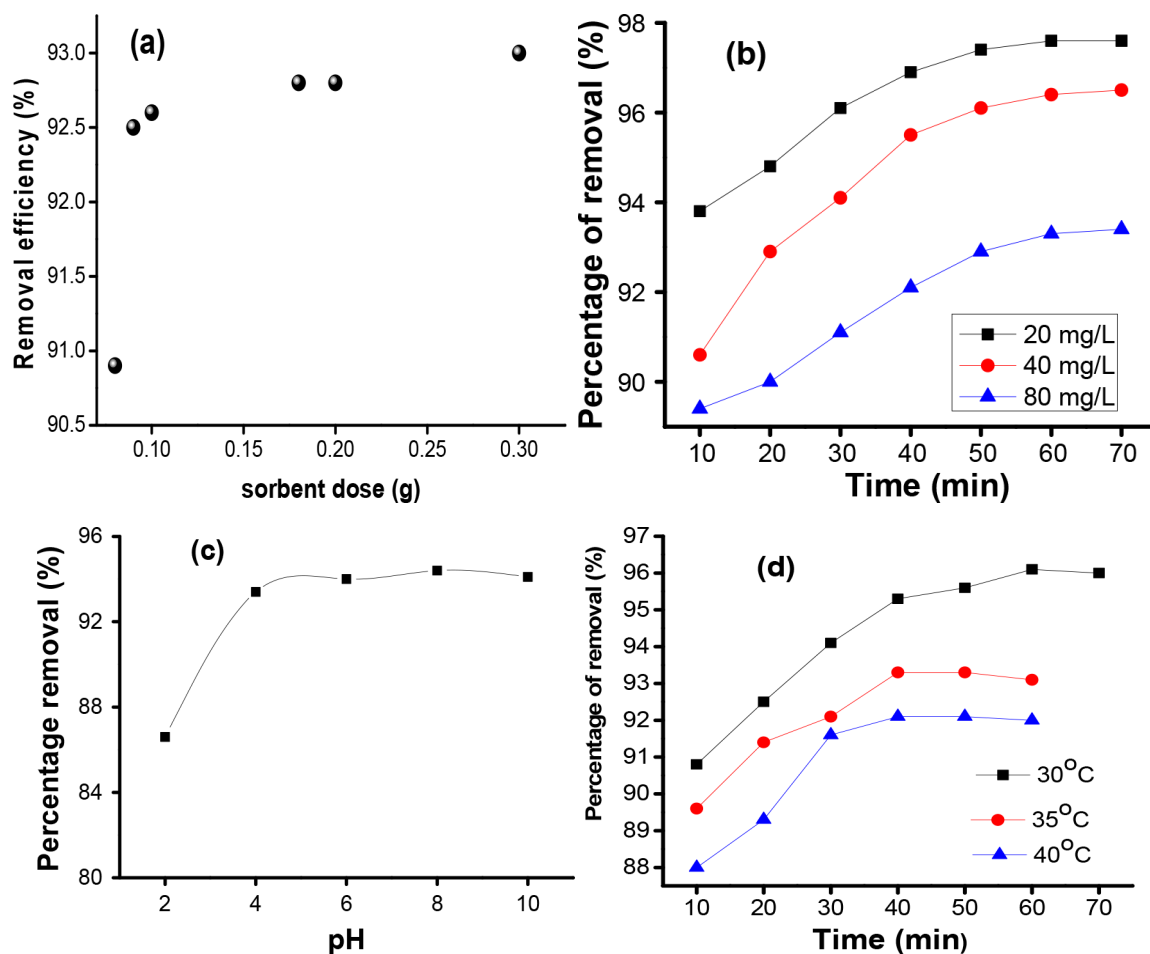


Fig. 2. (a) Effect of dose on removal of MB (b) effect of time on sorbed MB initial concentrations (c) effect of solution pH on MB removal (d) Effect of temperature on the removal (%) of MB by I-C (dosage = 0.18 g/70 mL; MB initial concentration = 80 mg L⁻¹).

Table 2

Comparison of maximum adsorption capacity (Q_m) of I-C for the adsorption of MB with different chitosan based adsorbents

Adsorbent	Temp (°C)	Dosage (g)	pH	Q_m (mg/g)	References
Iodate doped chitosan	25	0.18	8.0	108.7	This study
Chitosan-g-poly/montmorillonite		0.5	6.5	1859	[25]
Magnetic chitosan/graphene oxide		0.015	5.3	60.4	[26]
Cross-linked chitosan/sepiolite	30			40.99	[8]
α -chitin nanoparticles	–	–	–	6.90	[27]
Polyaniline nanotubes base	25	0.05	–	9.21	[28]
Liquefaction of spirulina (SP)		0.5	7	144.2	[29]
Kenaf core fibres	60			131.6	[30]
Walnut shell powder	318			51.55	[31]

are governed by exothermic process [21], similar results were reported in [22].

3.6. Adsorption isotherm

The isotherm models provide useful information about the interaction of the adsorbent surface and the dye. Adsorp-

tion isotherm experiments were carried out using varying concentrations of the dye (20, 40, 50, 70 and 80 mg/L), while the concentration of I-C was kept constant at 0.18 g/L. The experimental data were fitted by two Isotherm models of Freundlich and Langmuir [23] and are expressed in Eqs. (4) and (5), respectively. Furthermore, the Langmuir isotherm plot was expressed in terms of R_L , called separation factor,

which is defined by Eq. (6), and can be used to predict the feasibility of the adsorption process.

$$\frac{C_e}{q_e} = \frac{1}{q_m b} + \frac{C_e}{q_m} \quad (4)$$

$$\ln q_e = \ln k_f + \left(\frac{1}{n}\right) \ln C_e \quad (5)$$

$$R_L = \frac{1}{1 + bC_0} \quad (6)$$

where q_e is the amount of MB adsorbed at equilibrium per unit mass I-IC (mg/g), C_e is the equilibrium concentration of MB in solution (mg/L), q_m is the maximum mono layer adsorption capacity (mg/g), K_f is the adsorption capacity of the adsorbent in mg/g (L/mg)^{1/n} and stands for the amount of MB adsorbed onto the I-IC for a unit equilibrium concentration.

The values of the constants were determined from Eqs. (4), (5), and (6) respectively. The Freundlich and the Langmuir model constants, and their correlation coefficients, are listed in Table 3. It can be seen in Table 3 that the data were better fitted to the Langmuir model with R² value close to 1, signifying mono layer adsorption. Moreover, the values of R_L is < 1 indicating a favourable adsorption of MB on I-IC. The calculated monolayer adsorption capacity was 109 mg/g and significantly superior to those reported for similar adsorbents in literature (Table 2), thus showing a strong potential in the application of MB removal. The Freundlich constant (1/n) is indicative of the adsorption intensity of the adsorbent. When 1/n is less than 1.0, adsorption will readily take place. The values of 1/n for this study was 0.1548, this shows that the dye molecules were easily adsorbed onto the I-IC surface.

The superior capacity reported in this study may be attributed to the size of the developed pore and the incorporated iodate. The I-IC with a pores size of 21.7 nm, could have provided an excellent accessible pore structure and absorptive impact for the MB of molecular size 1.43 nm to easily penetrate and be retained.

3.7. Adsorption kinetics

Kinetic study of any adsorption process is important because it describes the uptake rates of the adsorbate and controls the residual time of the entire process [24]. To investigate the rate controlling step in the adsorption mechanism of the dye onto I-IC, both the Pseudo-first-order and pseudo-second order models were employed to deal with the data, as described in Eqs. (3) and (4), respectively,

$$\ln(q_e - q_t) = \ln q_e - k_1 t \quad (7)$$

$$\frac{t}{q_t} = \frac{1}{K_2 q_e^2} + \frac{1}{q_e} t \quad (8)$$

where q_e represents the equilibrium MB adsorption amount (mg/g), q_t represents the adsorption amount (mg/g) at contact time t (min) per unit mass I-IC, k_1 and k_2 are the adsorption rate constants for the pseudo first-order and pseudo second-order adsorption, respectively. The rate constants and other parameters obtained from the first and second order equations are summarized in Table 3. High determination coefficient (R² = 0.999) was obtained when the experimental data were fitted by pseudo-second order kinetic model indicating that the reaction rate depends on the number of active sites present on the surface. Besides, the calculated q_e value was in good agreement with the experimental data (q_e, exp), which suggests that the adsorption behaviour of MB by I-IC can be better described by pseudo-second-order kinetic model.

3.9. Adsorption thermodynamics

To estimate the effect temperature on the adsorption of dye on I-IC, thermodynamic parameters such as standard free energy (ΔG°), enthalpy ΔH° and entropy ΔS° were investigated. The change in free energy (ΔG°) was evaluated using Eq. (10) to examine the thermodynamic nature.

Table 3
Equilibrium, kinetic and thermodynamic parameters for MB adsorption onto I-IC

Equilibrium						
Langmuir			Freundlich			
Q_m (mg/g)	K (L/mg)	R_L	R ²	1/n	K_f (mg/g) (L /mg) ^{1/n}	R ²
108.7	0.6069	0.0202	0.9821	0.1548	0.6296	0.8613
Kinetics						
Pseudo-first -order			Pseudo-second-order			
Q_e exp. (mg/g)	Q_e cal (mg/g)	k_1 (min ⁻¹)	R ²	Q_e cal (mg/g)	k_2 (g/mg min)	R ²
38.5	1.355	0.026	0.7601	37.8	0.028	0.9995
Thermodynamic						
Temp (K)	ln K	ΔG° kJ/mol	ΔS° J/Kmol	ΔH° kJ/mol		
303	3.20	-8.061	78.20	- 31.59		
308	2.63	- 6.730				
313	2.44	-6.350				

$$\Delta G^\circ = -RT \ln K_c \quad (9)$$

ΔH° and ΔS° were calculated from Vant Hoff's equation as expressed below:

$$\ln K_c = \left(\frac{\Delta S^\circ}{R} \right) - \left(\frac{\Delta H^\circ}{R} \right) \frac{1}{T} \quad (10)$$

where K_c is the equilibrium constant, and R is the universal gas constant (8.314 J/mol K). The computed thermodynamic parameters are given in Table 3. The negative value of ΔH° indicates that the adsorption of MB on I-IC was exothermic. The value of K_c decreased by increasing temperature, which further affirms the exothermic nature of the adsorption process. The positive value of ΔS° is an indication of an increase in degree of freedom of the MB at the solid/liquid interface during the adsorption process and suggests good affinity of the MB towards I-IC [32]. The negative ΔG° values at all the investigated temperatures indicate the spontaneous nature of the adsorption of MB onto I-IC.

3.9. Regeneration of the adsorbent

To make the adsorption of MB on I-IC more economical, regeneration of the used adsorbent is of paramount importance. The result for desorption of MB using 70 mL of ethanol solution, 20 mg/L of MB and adsorbent dosage of 0.18 g is presented in Fig. 3. Total decrease in adsorption efficiency of I-IC for MB after three successful cycles was 0.0%, 1.3%, and 16.9%, respectively, which shows that I-IC has good potential to re-adsorb MB molecules from aqueous solution.

4. Conclusion

The present study involves the use of Iodate incorporated chitosan composite I-IC for MB removal from aqueous solution. The influences of adsorbent dose, contact time, pH and temperature on the removal of MB were studied. These

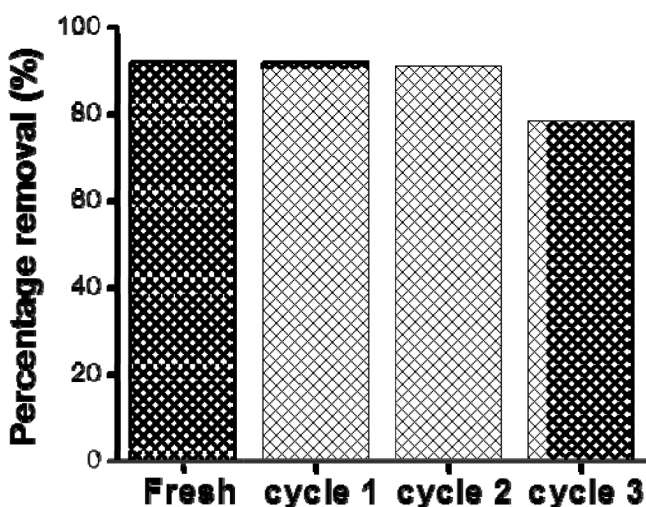


Fig. 3. Percentage of MB desorption from I-IC (80 min; MB = 20 mg/L; ads. dosage = 0.15 g/70 mL; temp. = $27 \pm 1^\circ\text{C}$).

results show that MB removal increases at increasing contact time, pH, I-IC dosage and comparably decreases with an increase in temperature. The I-IC exhibit high removal capacity (109 mg/g) towards the MB when compared to other adsorbents. The Pseudo-second order and Langmuir isotherm correlates the kinetic and the equilibrium date of MB adsorption onto I-IC better. The adsorbent show good reusability efficiency after three successive cycles. The results indicate that I-IC composite could be an efficient and potential adsorbent for the removal of methylene blue from aqueous solution and other cationic dyes.

Conflicts of interests

Authors have declared that no competing interests exist.

References

- [1] G. Moussavi, R. Khosravi, The removal of cationic dyes from aqueous solutions by adsorption onto pistachio hull waste, *Chem. Eng. Res. Des.*, 89 (2011) 2182–2189.
- [2] B. Sadhukhan, N.K. Mondal, S. Chattoraj, Biosorptive removal of cationic dye from aqueous system: A response surface methodological approach, *Clean Technol. Environ. Policy*, 16 (2014) 1015–1025.
- [3] M.T. Yagub, T.K. Sen, M. Ang, Removal of cationic dye methylene blue (MB) from aqueous solution by ground raw and base modified pine cone powder, *Environ. Earth Sci.*, 71 (2014) 1507–1519.
- [4] X. Chen, L. He, Microwave irradiation assisted preparation of chitosan composite micro sphere for dye adsorption, *Int. J. Polymer Sci.*, 2017 (2007) 1–8.
- [5] P. Wang, T. Yan, L. Wang, Removal of congo red from aqueous solution using magnetic chitosan composite micro particles, *Bio. Resour.*, 8 (2013) 6026–6043.
- [6] A.H. Gedam, R.S. Dongre, Adsorption characterization of Pb (II) ions onto iodate doped chitosan composite: equilibrium and kinetic studies, *RSC Adv.*, 5 (2015) 54188–54201.
- [7] Y. Li, Y. Zhou, W. Nie, L. Song, P. Chen, Highly efficient methylene blue dyes removal from aqueous systems by chitosan coated magnetic mesoporous silica nanoparticles, *J. Porous Mater.*, 22 (2015) 1383–1392.
- [8] F. Marrakchi, W.A. Khanday, M. Asif, B.H. Hameed, Cross-linked chitosan/sepiolite composite for the adsorption of methylene blue and reactive orange 16, *Int. J. Biol. Macromol.*, 93 (2016) 1231–1239.
- [9] L. Wang, J. Zhang, A. Wang, Fast removal of methylene blue from aqueous solution by adsorption onto chitosan-g-poly (acrylic acid)/attapulgite composite, *Desalination*, 266 (2011) 33–39.
- [10] N. Chubar, J.R. Carvalho, M.J.N. Correia, Heavy metals bio-sorption on cork biomass: Effect of the pre-treatment, *Colloids Surfaces A Physicochem. Eng. Asp.*, 238 (2004) 51–58.
- [11] F.A. Dawooda, K.G. Akpomiea, Simultaneous adsorption of Ni(II) and Mn (II) ions from aqueous solution onto a Nigerian kaolinite clay, *J. mater. Res. Technol.*, 3 (2014) 129–141.
- [12] C. Karen, P. Junior, C. Vitor, Magnetic activated carbon derived from biomass waste by concurrent synthesis: efficient adsorbent for toxic dyes, *ACS Sustain. Chem. Eng.*, 4 (2016) 1058–1068.
- [13] M.A. Brown, Z. Liu, P.D. Ashby, A. Mehta, R.L. Grimm, J.C. Hemminger, Surface structure of KIO_3 grown by heterogeneous reaction of ozone with KI (001), *J. Phys. Chem. C.*, 112 (2008) 18287–18290.
- [14] Udayabhanu, G. Nagaraju, H. Nagabhushana, R.B. Basavaraj, G.K. Raghu, D. Suresh, H. Rajanaika, S.C. Sharma, Green, non chemical route for the synthesis of ZnO superstructures, evaluation of its applications towards photo catalysis, photoluminescence and bio-sensing, *Cryst. Growth Des.*, 16 (2016) 6828–6840.

- [15] H. Manghabati, G. Pazuki, A study on the decolorization of methylene blue by *Spirodela polyrrhiza*: experimentation and modeling, *Rsc Adv.*, 4 (2014) 30137–30144.
- [16] L. Zhang, Q. Liu, P. Hu, R. Huang, Adsorptive removal of methyl orange using enhanced cross-linked chitosan/bentonite composite, *Desal. Water Treat.*, 57 (2016) 17011–17022.
- [17] Y. Gao, S. Xu, Q. Yue, Y. Wu, B. Gao, Chemical preparation of crab shell-based activated carbon with superior adsorption performance for dye removal from wastewater, *J. Taiwan Inst. Chem. Eng.*, 61 (2016) 327–335.
- [18] R. Gong, J. Ye, W. Dai, X. Yan, J. Hu, X. Hu, S. Li, H. Huang, Adsorptive removal of methyl orange and methylene blue from aqueous solution with finger-citron-residue-based activated carbon, *Ind. Eng. Chem. Res.*, 52 (2013) 14297–14303.
- [19] M.I. Khan, T.K. Min, K. Azizli, S. Sufian, H. Ullah, Z. Man, Effective removal of methylene blue from water using phosphoric acid based geopolymers: Synthesis, characterizations and adsorption studies, *RSC Adv.*, 5 (2015) 61410–61420.
- [20] Y. Bulut, H. Karaer, Adsorption of methylene blue from aqueous solution by cross linked chitosan/bentonite composite, *J. Dispers. Sci. Technol.*, 36 (2014) 61–67.
- [21] Y.C. Sharma, Adsorption characteristics of a low-cost activated carbon for the reclamation of colored effluents containing malachite green, *J. Chem. Eng. Data*, 56 (2011) 478–484.
- [22] S. Mahiya, S.K. Sharma, G. Lofrano, Adsorptive behavior, isothermal studies and kinetic modeling involved in removal of divalent lead from aqueous solutions, using *Carissa carandas* and *Syzygium aromaticum*, *Cogent Environ. Sci.*, 2 (2016) 1–12.
- [23] R. Mallampati, L. Xuanjun, A. Adin, S. Valiyaveetil, Fruit peels as efficient renewable adsorbents for removal of dissolved heavy metals and dyes from water, *ACS Sustain. Chem. Eng.*, 3 (2015) 1117–1124.
- [24] M. Abbas, M. Trari, Kinetic equilibrium and thermodynamic study on the removal of Congo Red from aqueous solutions by adsorption onto apricot stone, *Process Safety Environ. Protect.*, 8 (2015) 424–436.
- [25] L. Wang, J. Zhang, A. Wang, Removal of methylene blue from aqueous solution using chitosan- g -poly (acrylic acid)/montmorillonite super adsorbent nanocomposite, *Colloids Surf. A: Physicochem. Eng.*, 322 (2008) 47–53.
- [26] L. Fan, C. Luo, X. Li, F. Lu, H. Qiu, M. Sun, Fabrication of novel magnetic chitosan grafted with graphene oxide to enhance adsorption properties for methyl blue, *J. Hazard. Mater.*, 215–216 (2012) 272–279.
- [27] S. Dhananasekaran, R. Palanivel, S. Pappu, Adsorption of methylene blue, bromophenol blue, and coomassie brilliant blue by α -chitin nanoparticles, *J. Adv. Res.*, 7 (2016) 113–124.
- [28] M.M. Ayad, A.A. El-nasr, Adsorption of cationic dye (methylene blue) from water using polyaniline nanotubes base, *J. Phys. Chem. C.*, 114 (2010) 14377–14383.
- [29] L. Leng, X. Yuan, H. Huang, H. Wang, Z. Wu, L. Fu, X. Peng, X. Chen, G. Zeng, Characterization and application of bio-chars from liquefaction of micro algae, lignocellulosic biomass and sewage sludge, *Fuel Process. Technol.*, 129 (2015) 8–14.
- [30] M.S. Sajab, M.K.A.C.H.C.S.Z. Saad Mohd Jani, W.S.C.K.L.C. Poi Sim Khiew, Citric acid modified kenaf core fibres for removal of methylene blue from aqueous solution, *Bioresour. Technol.*, 102 (2011) 7237–7243.
- [31] R. Tang, C. Dai, C. Li, W. Liu, S. Gao, C. Wang, Removal of methylene blue from aqueous solution using agricultural residue walnut shell: equilibrium, kinetic, and thermodynamic studies, *J. Chem.*, 2017.
- [32] L. Ai, M. Li, L. Li, Adsorption of methylene blue from aqueous solution with activated carbon/cobalt ferrite/alginate composite beads : kinetics, isotherms, and thermodynamics, *J. Chem. Eng. Data*, 34 (2011) 134–143.